Effects of Ca doping on the crystallization kinetics of GeTe

Chenfei Wang,[1] Guanjun Yao,[1] Juncheng Liu,[1] Yuanen Mao,[2] Wenhao Leng,[2] Yimin Chen,[1,2,a] Xiang Shen,[2] Jun-Qiang Wang,[3] and Rongping Wang[2,b]

AFFILIATIONS

[1]Department of Microelectronic Science and Engineering, School of Physical Science and Technology, Ningbo University, Ningbo 315211, China

[2]Laboratory of Infrared Material and Devices and Key Laboratory of Photoelectric Materials and Devices of Zhejiang Province, Advanced Technology Research Institute, Ningbo University, Ningbo 315211, China

[3]CAS Key Laboratory of Magnetic Materials and Devices and Zhejiang Province Key Laboratory of Magnetic Materials and Application Technology, Ningbo Institute of Materials Technology and Engineering, Chinese Academy of Sciences, Ningbo 315201, China

[a]Author to whom correspondence should be addressed: chenyimin@nbu.edu.cn
[b]wangrongping@nbu.edu.cn

ABSTRACT

Doping is an effective way to improve the performance of conventional phase-change materials. We introduced an alkaline element calcium (Ca) in GeTe films and studied their crystallization kinetics by using flash DSC. It was found that a small amount of Ca doping (4.0 at. %) can significantly enhance the thermal stability, but the maximum crystal growth rate does not decrease significantly. Moreover, no any Ca-related crystalline phase and Ca-related chemical bond can be found in Ca-doped GeTe, implying that Ca atoms are in free state in GeTe matrix.

Published under an exclusive license by AIP Publishing. https://doi.org/10.1063/5.0051288

Phase-change memory based on the Ovshinsky effect[1] nowadays is becoming one of the most potential candidates for the next generation of nonvolatile memory, which thanks to its large-scale integration, low power consumption, good data retention ability, fast operation speed, and the excellent compatibility with complementary metal oxide semiconductor technology. Phase-change memory is also promising as "in computing" memory to overcome the data traffic bottleneck between central processing units and memory units. Recently, a concept of "neuro-morphological computing" has been proposed in the field of phase-change memory, and many works have focused on the so-called phase-change neuro-inspired devices.[2–4]

It is noted that the super-high integration and ultra-fast information processing in phase-change neuro cells depend on the excellent amorphous thermal stability and rapid crystallization rate in phase-change materials (PCMs), respectively. Therefore, the crystallization kinetics of PCMs that can be used to quantitatively estimate thermal stability and crystallization rate must be performed before designing phase-change neuro cells.[5] An ultra-fast differential scanning calorimetry named Flash DSC has been employed to study the crystallization kinetics of PCMs. In combination with suitable viscosity model and the Kissinger method, many conventional PCMs, such as the $Ge_2Sb_2Te_5$ (GST),[6] $Ag_{5.5}In_{6.5}Sb_{29}Te_{59}$ (AIST),[7] and GeTe,[8] were confirmed to have fast crystallization rate approaching their melting temperature (T_m). Rao et al. designed $Sc_{0.2}Sb_2Te_3$-based PCMs with a sub-nanosecond operation speed[9] and demonstrated that the $Sc_{0.2}Sb_2Te_3$ has fast crystal growth rate at 0.73 T_m.[10] However, the amorphous thermal stability of such PCMs is not good enough to meet the requirement of the phase-change neuro application at all.

In the previous work, we introduced an alkaline element calcium (Ca) in GST but no significant enhancement of amorphous thermal stability was found even in the film with the moderate Ca concentration of 6.4 at. %, and thus, we did not study the crystallization kinetics of Ca-doped GST.[11] Since GeTe has better thermal stability than GST, in this work, we prepared Ca-doped GeTe films and investigated their crystallization kinetics by Flash DSC. It was found that Ca atoms (with a concentration of 4.0 at. %), which are in the free state and may occupy the vacancy sites in GeTe matrix, can significantly enhance the
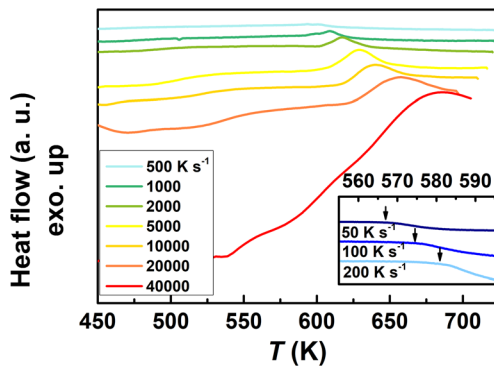
FIG. 1. The Flash DSC traces of GTC with different heating rate. The inset is an enlarged figure of the main panel for the DSC traces at low heating rates where the black arrows indicate the value of their respective T_p.

thermal stability without sacrificing the maximum crystal growth rate very much.

GeTe (GT) and $Ca_{4.0}(GeTe)_{96.0}$ (GTC) films with a thickness of ~200 nm were deposited on $SiO_2/Si(100)$ and NaCl(100) substrates by the magnetron sputtering method at a room temperature. A single GeTe target was installed on DC source with a sputtering power of 50 W to obtain the pure GeTe films. The separated GeTe and Ca targets were installed on DC and RF source, respectively, with the sputtering power of 50 W and 27 W, to prepare the $Ca_{4.0}(GeTe)_{96.0}$ films. Finally, another thin SiO_2 layer (about 5 nm) was deposited on the top of each film using a single SiO_2 target with a RF power of 20 W and a deposition time of 5 min to prevent the possible surface oxidation. The background pressure was less than 5.0×10^{-5} Pa, and the sputtering pressure was set to 0.4 Pa with Ar gas flow. The compositions of these films were examined by energy dispersive spectroscopy (EDS, Tescan Vega 3SBH), and they are $Ge_{48.43}Te_{51.57}$ and $Ge_{46.52}Te_{49.50}Ca_{3.98}$, respectively. The films were annealed at different temperatures by using a rapid annealing furnace with a heating rate of 100 K s^{-1} in N_2 gas flow. Amorphous/crystalline structures and crystallization behaviors of these films were studied by using x-ray diffraction (XRD,

Bruker D2 PHASER diffractometer, with the Cu/Kα radiation wavelength of 0.15405 nm) and Raman spectroscopy (Renishaw inVia, with the pump laser of 785 nm). The chemical bonding information in GeTe and $Ca_{4.0}(GeTe)_{96.0}$ was investigated by x-ray photoelectron spectroscopy (XPS, Thermo Scientific K-Alpha$^+$). The non-isothermal calorimetry was performed by flash differential scanning calorimetry (Flash DSC, Mettler Toledo Flash DSC 1), which had a fast scanning rate more than 40 000 K s^{-1} and high measurement precision, to study the crystallization kinetics of phase-change materials. The film deposited on NaCl (100) substrate was easily removed in distilled water, and thus dozens of nanogram materials can be obtained for Flash DSC measurements.

We first performed the flash DSC to study the crystallization kinetics of GT and GTC films. Figure 1 is the typical Flash DSC traces of GTC. With the increase in heating rate from 50 to 40 000 K s^{-1}, T_p (the temperature of exothermic peak in Fig. 1) increases from 566 to 687 K. The Flash DSC traces of GT were also measured but not exhibited here. T_p values of GT and GTC were plotted in Fig. 2(a) by using the Kissinger equation as follows:

$$ ln\left(\frac{\varnothing}{T_P^2}\right) = -\frac{Q}{R\,T_P} + A, \qquad (1) $$

where Q is the activation energy for crystallization, R is the ideal gas constant (8.314 J mol^{-1} K^{-1}), A is a constant, and ϕ is the heating rate. All the Q values of GT and GTC decrease obviously when the temperature increases, implying a strong non-Arrhenius behavior in these phase-change supercooled liquids.

Henderson believed that, when the T_p is equal to the temperature at which the crystallization fraction is 63% ($T_{0.63}$), it is reliable using Kissinger method to estimate the crystallization kinetics.[12] This assumption is also valid to study the crystallization kinetics in phase-change materials.[13] Together with the generalized Mauro–Yue–Ellison–Gupta–Allan (g-MYEGA) viscosity model, we first performed Johnson–Mehl–Avrami (JMA) numerical simulation, which was widely used in previous works,[8,14–17] to approximate the heating process with the same scanning rate in Fig. 1. It was found that T_p values obtained from numerical simulated traces are in accord with those
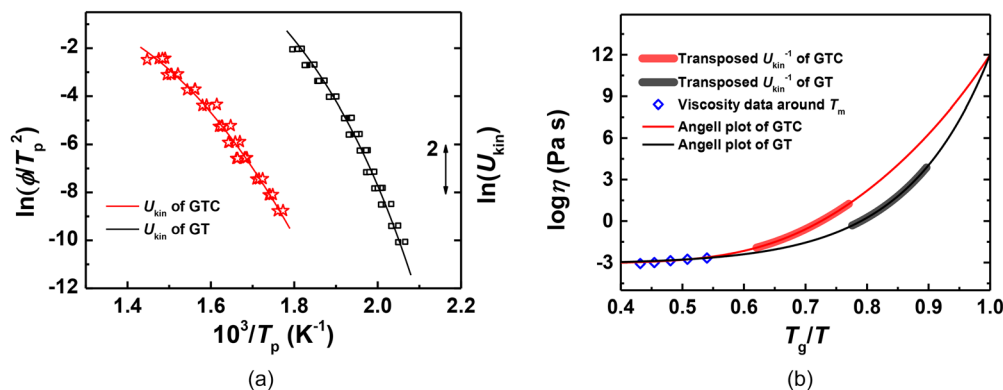
FIG. 2. (a) Kissinger plots of GT and GTC. The hollow squares and starts represent the flash DSC data for GT and GTC, respectively. The curves represent the related crystallization kinetics coefficient U_{kin} that are fitted by the g-MYEGA viscosity model. (b) Angell plots of GT and GTC. The glass transition temperature (T_g) of GT is 432.1 K.[8] The T_g of GTC is also set to 432.1 K because of the less amount Ca doping. The thin blue and black curves are the Angell plots of GT and GTC fitted by g-MYEGA viscosity model. The thick curves indicate the Flash DSC measurement temperature region. The hollow rhombuses represent the viscosity data of GT around T_m.[18].

TABLE I. The fitted parameters and some crystallization kinetics parameters of GT and GTC.

PCMs	C	W_1 (K)	W_2 (K)	C_1 (K)	C_2 (K)	η_∞ (Pa s)	$T_{f\text{-s}}$ (K)	f	m
GT	−1.0	0.048	0.048	2782	2782	$10^{-3.08}$	…	…	112
GTC	−2.8	2.272	0.00328	5559	1340	$10^{-3.06}$	645	1.07	67

obtained from the measured traces in each heating rate, implying simulated DSC traces can be used to confirm the validities of the Kissinger method in the crystallization kinetics study of GT and GTC supercooled liquids. We then compared the difference between T_p and $T_{0.63}$, and found that there is no obvious divergence even at the highest heating rate of 40 000 K s^{-1} (the difference is less than 1 K). This supports us to study the crystallization kinetics further based on the Kissinger results in Fig. 2(a).

The crystallization kinetics coefficient U_{kin} and viscosity η can be transposed each other by using Stokes–Einstein relation,[19]

$$\log_{10} U_{kin} = C - \log_{10}\eta, \qquad (2)$$

where C is a constant. The temperature dependent viscosity η can be depicted by g-MYEGA viscosity model,[20]

$$\log_{10}\eta = \log_{10}\eta_\infty + \frac{1}{T\left[W_1\exp\left(-\dfrac{C_1}{T}\right) + W_2\exp\left(-\dfrac{C_2}{T}\right)\right]}, \qquad (3)$$

where η_∞ is the viscosity at infinite high temperature and all W_1, W_2, C_1, and C_2 are the temperature related constants. Replacing Eq. (3) into Eq. (2), the U_{kin} can be expressed as follows:

$$\log_{10} U_{kin} = C - \log_{10}\eta_\infty - \frac{1}{T\left[W_1\exp\left(-\dfrac{C_1}{T}\right) + W_2\exp\left(-\dfrac{C_2}{T}\right)\right]}. \qquad (4)$$

Employing this expression, the relative U_{kin} can be obtained as shown in Fig. 2(a). The fitted parameters are listed in Table I. As we see that GT has the values of $W_1 = W_2$ and $C_1 = C_2$, while GTC has fitted values of $W_1 \neq W_2$ and $C_1 \neq C_2$, indicating nonexistence and existence of fragile-to-strong (FS) transition in the respective supercooled liquid. We estimated the FS temperature ($T_{f\text{-s}}$) by the following expression:

$$T_{fs} = \frac{C_1 - C_2}{\ln W_1 - \ln W_2}. \qquad (5)$$

It yields the $T_{f\text{-s}}$ of 645 K for GTC. However, the FS transition magnitude (f) is just 1.07, which is very close to 1 ($f = 1$ means no FS transition). Such results can also be found in the Angell plots as shown in Fig. 2(b). Compared with the results in Zn–Sb–Te film reported before,[17] there is no distinct FS transition in GT and GTC studied here. Another important crystallization kinetics parameter, the supercooled liquid fragility m can be calculated by the following equation:[21]

$$m = \left[\partial\log_{10}\eta / \partial\left(T/T_g\right)\right]_{T=T_g}. \qquad (6)$$

It yields the m is 112 and 67 for GT and GTC, respectively. The value of fragility index of GeTe has been already reported in the previous work,[19] and it is also in accord with the result estimated by Sosso et al.

with large-scale molecular dynamics (m is 111 for GeTe).[22] The fragility index of $Ca_{4.0}(GeTe)_{96.0}$ is lower than that of GST ($m = 90$) but similar to that of Ge_7Sb_{93} ($m = 65$).[6,23] As we can see that although the less amount of Ca doping could not induce any distinct FS transition in the supercooled liquids, the value of m is significantly decreased, indicating that a stronger structure (near T_g) is built with doping. This is also the interpretation for the enhancement of amorphous thermal stability in GeTe by a small amount Ca doping.

Considering that the crystal growth is mainly governed by the diffusion processes at the crystal–liquid interface in phase-change supercooled liquids, the absolute value of U_{kin} at T_m can be estimated by the Stokes–Einstein relationship.[6] With T_m of 1000 K and the corresponding viscosity of $1 \times 10^{-3.008}$ Pa s, the absolute value of U_{kin} at T_m was calculated as 16.57 m s^{-1}. According to this absolute value, we adjusted the temperature dependent U_{kin} that was depicted in Fig. 2(a) to be absolute one. Then, the temperature dependent crystal growth rate U can be extrapolated by the following expression:[24]

$$U = U_{kin}\left[1 - \exp\left(-\frac{\Delta G}{RT}\right)\right], \qquad (7)$$

where R is the ideal gas constant (8.314 J mol^{-1} K^{-1}) and ΔG is the driving force of crystallization. For chalcogenide supercooled liquids of PCMs, the ΔG obeys the following expression:[25]

$$\Delta G = \frac{\Delta H_m(T_m - T)}{T_m}\left(\frac{2T}{T_m + T}\right), \qquad (8)$$

where ΔH_m is melting latent heat, being 17.9 kJ mol^{-1} for both GT and GTC. We finally extrapolated and obtained the reduced temperature dependent U in the supercooled temperature range (T_g to T_m) as shown in Fig. 3. The extrapolated results of GeTe are in good agreement with the crystal growth rates estimated by the methods of optical reflection,[26] in situ TEM,[8] and dynamic TEM,[27] in both high and low temperatures. Compared with the extrapolated U of GT, the U of GTC significantly decreases as the temperature far away from T_m, i.e., the U of GTC is about three orders of magnitude lower than that of GT when the temperature is 0.5 T_m. This result supports the conclusions that less amount Ca doping can enhance thermal stability very well. Moreover, in the inset of Fig. 3, the maximum crystal growth rate (U_{max}) of GTC is 3.14 m s^{-1} at 0.84 T_m, which is very close to that of GT (3.55 m s^{-1} at 0.82 T_m), indicating that the fast crystal growth rate of GT is insignificantly decreased by the small amount of Ca doping.

From the crystallization kinetics results mentioned above, we concluded that the small amount of Ca doping (4.0 at. %) in GeTe can enhance the thermal stability significantly near T_g without sacrificing the crystal growth rate very much near T_m. The question, therefore, moves to that why the small amount doping can make such prominent effects on the crystallization kinetics. Thus, we further investigated the amorphous and crystalline structures of GT and GTC by using XRD, Raman, and XPS.
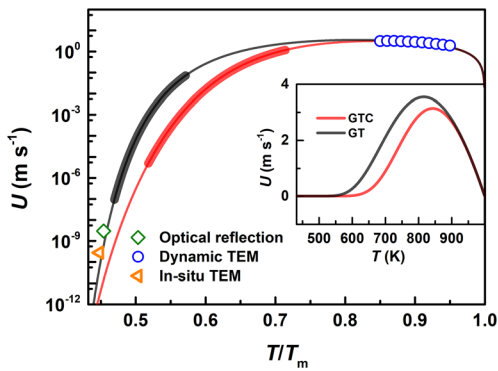
FIG. 3. Reduced temperature (T/T_m) dependences of crystal growth rate for GT and GTC supercooled liquids with logarithmic plot. The thick curves are the flash DSC measurement temperature range. The green rhombus, bule cycle, and orange triangle are the crystal growth rate measured by optical reflection,[26] dynamic TEM,[27] and *in situ* TEM,[6] respectively. The inset is the temperature dependent crystal growth rate with linear plot.

Figures 4(a) and 4(b) show the XRD patterns of GT and GTC films, respectively. As we see that, there is no sharp diffraction peak in the as-deposited films, implying all the as-deposited films are amorphous. Three distinct diffraction peaks of (021), (202), and (220), which belong to GeTe crystalline phase, can be found in 513 K and 573 K annealed GT. Following the standard PDF card (No. 7–125) from JCPDS-ICDD (International Center for Diffraction Data) in 2004, here we labeled the Miller indices in Figs. 4(a) and 4(b). The crystalline GeTe phase is distorted NaCl structure, and the corresponding space group is R3m, which are in line with the reported results.[28] Such diffraction peaks could not be found in 513 K annealed GTC film because only amorphous state was shown in this film, but they were found in 573 K annealed GTC film due to the presence of crystalline structure. Figures 4(c) and 4(d) show the Raman spectra of GT and GTC. Four bands of A, B, C, and D, which are located at 77, 125, 160, and 221 cm^{-1}, respectively, can be found in the as-deposited films. These bands are the typical Raman shifts of amorphous GeTe,[29] indicating that the as-deposited films are all amorphous. It was found that two new peaks located at 87 (peak E) and 118 cm^{-1} (peak F), which are the typical Raman peaks of crystalline GeTe, are presented in 513 K and 573 K annealed GT films. However, there are A, B, C,
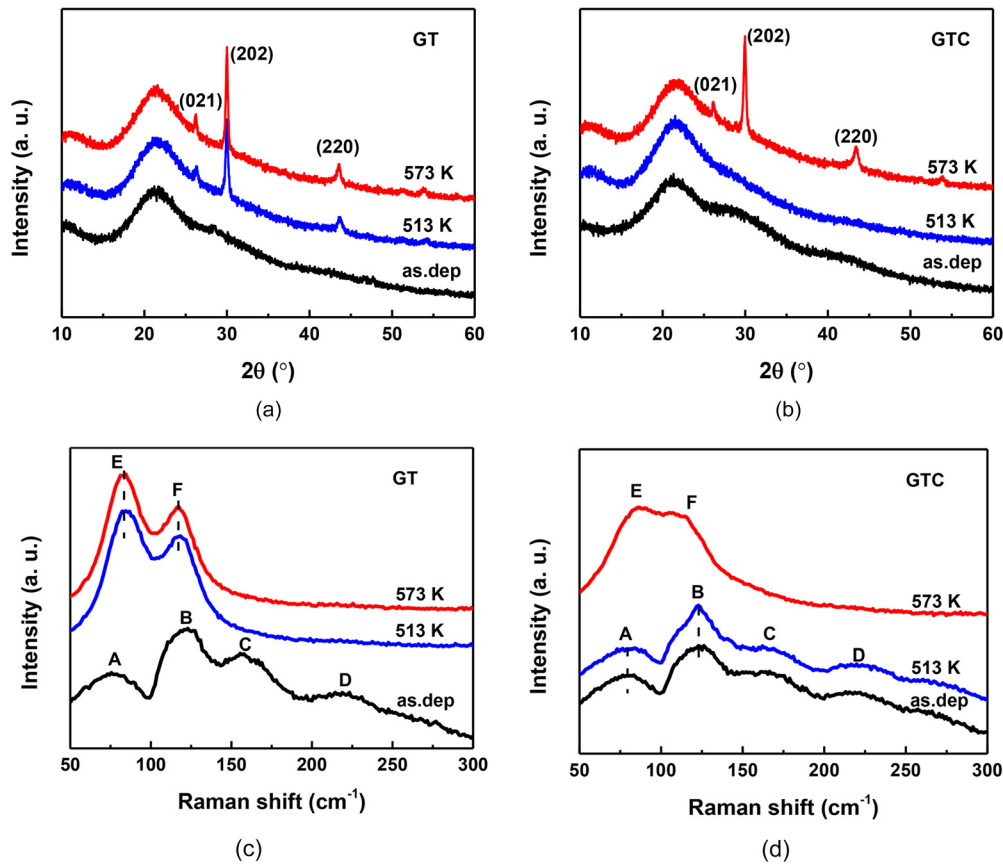
FIG. 4. XRD patterns of as-deposited, 513 K annealed, 573 K annealed (a) GT and (b) GTC films. Raman spectra of as-deposited, 513 K annealed, 573 K annealed (c) GT, and (d) GTC films.
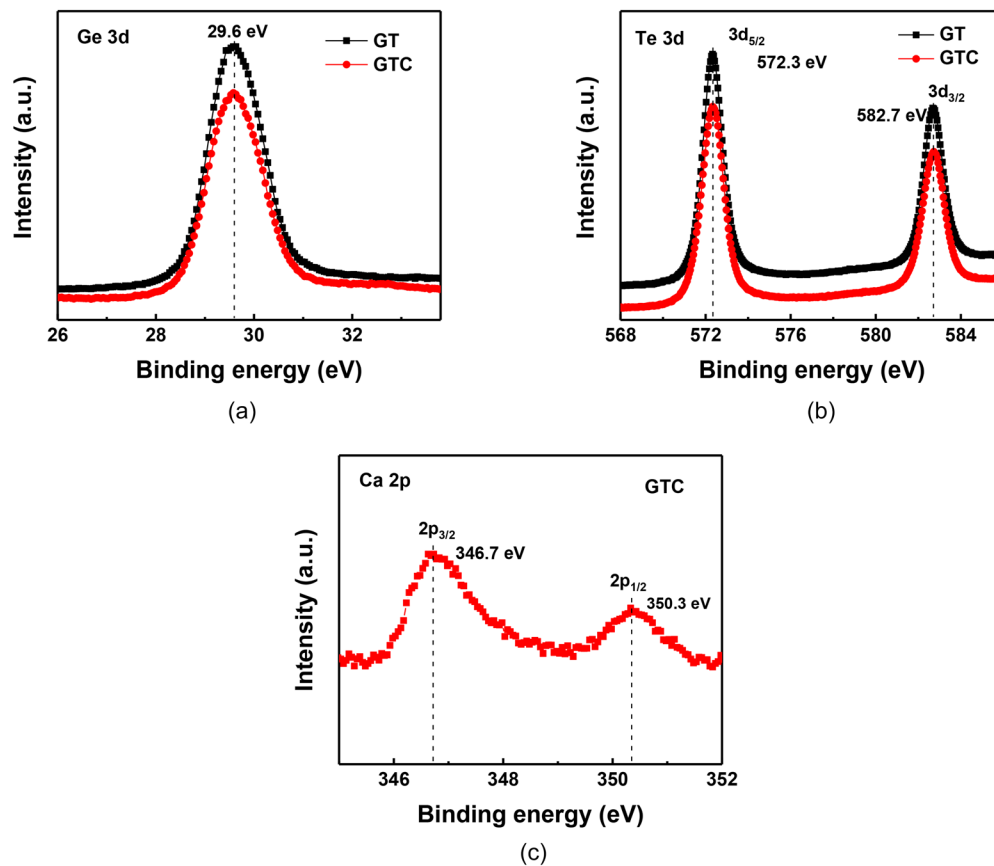
FIG. 5. The XPS spectra of (a) Ge 3d, (b) Te 3d, (c) Ca 2p, for GT and GTC films.

and D peaks in 513 K annealed GTC film and E, F peaks in 573 K annealed GTC film. These evidence are in good agreement with the XRD results and strongly support that the less amount of Ca doping can significantly enhance the thermal stability of GeTe without any dopant Ca-related phase separates out.

It is clear that there is no Ca-related crystalline phase in the matrix of GTC. Thus, it is arguable whether Ca-related chemical bonds can be formed in amorphous GTC matrix to affect the crystallization kinetics? We then performed XPS measurements to solve this argument. In order to distinguish the possible effect of surface oxidation and 5 nm thick SiO_2 layer, a surface layer with the thickness of $\sim$20 nm was removed from the film by ion sputtering before the XPS measurements. Figure 5 shows the XPS spectra of the as-deposited GT and GTC films. For GT, the binding energy of Ge 3d, Te $3d_{5/2}$, and Te $3d_{3/2}$, is 29.6, 572.3, and 582.7 eV, respectively. For GTC, the same binding energies can be found, indicating less amount of Ca doping could not change the chemical surroundings in the matrix of GT. In other words, there is no Ca-Ge and/or Ca-Te bonds in GTC film. Moreover, the binding energy of Ca $2p_{3/2}$ and Ca $2p_{1/2}$ can be found as 346.7 and 350.3 eV, respectively, in GTC film. Such binding energies are in agreement with the values for bulk material or elemental Ca, which are tabulated in the XPS handbook.[30]

Together with all the results above, it is believed that Ca atoms are in the free states in GeTe matrix, which is similar to the Ca element in GST.[11] Some of the vacancies in GeTe, which is the key for fast crystallization and good thermal stability in PCMs, might be occupied by these Ca atoms and then affects the crystallization kinetics.

In summary, we studied the effects of small amount Ca doping (4.0 at. %) on the crystallization kinetics of conventional GeTe PCMs by the Flash DSC. It was found that the doping can significantly enhance the thermal stability near T_g (the U of $Ca_{4.0}(GeTe)_{96.0}$ is one or two of magnitudes lower than that of GeTe) without sacrificing much crystallization rate near T_m (the U_{max} of $Ca_{4.0}(GeTe)_{96.0}$ and GeTe is 3.14 and 3.55 m s^{-1}, respectively). The supercooled fragility m decreases from 112 to 67, indicating the weak structure of GeTe near T_g becomes moderate strong one. Moreover, from XRD, Raman, and XPS measurements, no Ca-related crystalline phase and Ca-related chemical bonds can be found in $Ca_{4.0}(GeTe)_{96.0}$ matrix. This implies that the small amount of Ca is in the free state in GeTe matrix.

DATA AVAILABILITY

The data that support the findings of this study are available from the corresponding author upon reasonable request.

REFERENCES

[1]S. R. Ovshinsky, Phys. Rev. Lett. **21**, 1450 (1968).

[2]W. Zhang, R. Mazzarello, M. Wuttig, and E. Ma, Nat. Rev. Mater. **4**, 150 (2019).

[3]T. Tuma, A. Pantazi, M. L. Gallo, A. Sebastian, and E. Eleftheriou, Nat. Nanotechnol. **11**, 693 (2016).

[4]A. Sebastian, T. Tuma, N. Papandreou, M. L. Gallo, L. Kull, T. Parnell, and E. Eleftheriou, Nat. Commun. **8**, 1115 (2017).

[5]A. Sebastian, M. L. Gallo, and D. Kreb, Nat. Commun. **5**, 4314 (2014).

[6]J. Orava, A. L. Greer, B. Gholipour, D. W. Hewak, and C. E. Smith, Nat. Mater. **11**, 279 (2012).

[7]J. Orava, D. W. Hewak, and A. L. Greer, Adv. Funct. Mater. **25**, 4851 (2015).

[8]Y. Chen, G. Wang, L. Song, X. Shen, J. Wang, J. Huo, R. Wang, T. Xu, S. Dai, and Q. Nie, Cryst. Growth Des. **17**, 3687 (2017).

[9]F. Rao, K. Ding, Y. Zhou, Y. Zheng, M. Xia, S. Lv, Z. Song, S. Feng, I. Ronneberger, R. Mazzarello, W. Zhang, and E. Ma, Science **358**, 1423 (2017).

[10]B. Chen, Y. Chen, K. Ding, K. Li, F. Jiao, L. Wang, X. Zeng, J. Wang, X. Shen, W. Zhang, F. Rao, and E. Ma, Chem. Mater. **31**, 8794 (2019).

[11]Y. Mao, Y. Chen, Q. Zhang, R. Wang, and X. Shen, J. Non-Cryst. Solids **549**, 120338 (2020).

[12]D. W. Henderson, J. Non-Cryst. Solids **30**, 301 (1979).

[13]J. Orava and A. L. Greer, Thermochim. Acta **603**, 63 (2015).

[14]Y. Chen, Q. Li, Z. Yang, X. Shen, X. Wang, R. Wang, and M. Zhang, J. Am. Ceram. Soc. **103**, 1593 (2020).

[15]Y. Chen, J. Gu, Q. Zhang, Y. Mao, G. Wang, R. Wang, X. Shen, J.-Q. Wang, and T. Xu, Phys. Rev. Mater. **4**, 033403 (2020).

[16]Y. Chen, H. Pan, S. Mu, G. Wang, R. Wang, X. Shen, J. Wang, S. Dai, and T. Xu, Acta Mater. **164**, 473 (2019).

[17]J. Gu, Y. Chen, Q. Zhang, G. Wang, R. Wang, X. Shen, J. Wang, and T. Xu, Appl. Phys. Lett. **115**, 091903 (2019).

[18]G. C. Sosso, J. Behler, and M. Bernasconi, Phys. Status Solidi A **213**, 329 (2016).

[19]Q. Zhang, Y. Chen, W. Leng, J. Gu, Y. Mao, X. Shen, R. Wang, T. Xu, J.-Q. Wang, and G. Wang, Scr. Mater. **192**, 89 (2021).

[20]C. Zhang, L. Hu, Y. Yue, and J. C. Mauro, J. Chem. Phys. **133**, 014508 (2010).

[21]C. A. Angell, MRS Bull. **33**, 544 (2008).

[22]G. C. Sosso, J. Behler, and M. Bernasconi, Phys. Status Solidi B **249**, 1880 (2012).

[23]B. Chen, J. Momand, P. A. Vermeulen, and B. J. Kooi, Cryst. Growth Des. **16**, 242 (2016).

[24]M. Ediger, P. Harrowell, and L. Yu, J. Chem. Phys. **128**, 034709 (2008).

[25]L. Battezzati and A. Greer, J. Mater. Res. **3**, 570 (1988).

[26]M. Libera and M. Chen, J. Appl. Phys. **73**, 2272 (1993).

[27]M. K. Santala, B. W. Reed, S. Raoux, T. Topuria, T. LaGrange, and G. H. Campbell, Appl. Phys. Lett. **102**, 174105 (2013).

[28]M. Upadhyay, S. Murugavel, M. Anbarasu, and T. R. Ravindran, J. Appl. Phys. **110**, 083711 (2011).

[29]K. S. Andrikopoulos, S. N. Yannopoulos, G. A. Voyiatzis, A. V. Kolobov, M. Ribes, and J. Tominaga, J. Phys.: Condens. Matter **18**, 965 (2006).

[30]J. F. Moulder, W. F. Stickle, P. E. Soboc, and K. D. Bomben, *Handbook of X-ray Photoelectron Spectroscopy* (Physical Electronics, USA, 1992).